Supplementary Information

Chemically or physically introducing lipids to lysine-histidine-based peptide systems for safe, efficient and targeted mRNA delivery

Chuanmei Tang,[a,‡] *Yuzhi Ye,*[a,‡] *Yaohui Du,*[a] *Yulin Sun,*[a] *Rongxin Su,*[a,b,c] *Wei Qi*[a,b,c,*] *and Yuefei Wang*[a,c,*]

[a] State Key Laboratory of Chemical Engineering and Low-Carbon Technology, School of Chemical Engineering and Technology, Tianjin University, Tianjin 300072, P. R. China

[b] Collaborative Innovation Center of Chemical Science and Engineering (Tianjin), Tianjin 300072, P. R. China

[c] Tianjin Key Laboratory of Membrane Science and Desalination Technology, Tianjin University, Tianjin 300072, P. R. China.

*Corresponding author: Wei Qi (email: qiwei@tju.edu.cn), Yuefei Wang (email: wangyuefei@tju.edu.cn)

‡These authors contributed equally.

Supplemental Experimental Procedures

Chemicals and materials. KHn (>98%, desalted) were synthesized by GL Biochem Ltd. (Shanghai, China) (**Table S1**). 1, 2-epoxides (labeled as Ax or Ex, A is for alkanol and E is for enol, *x* is the number of carbon ranging from 10 to 18) were all purchased from Tokyo Chemical Industry (TCI). 1,2-dioleoyl-3-trimethylammonium-propane (DOTAP) was obtained from Avanti Polar Lipids. Commercial transfection reagent Lipofectamine 2000 (Lipo 2000) was purchased from Thermo Fisher Scientific. The enhanced green fluorescent protein (EGFP) mRNA (mEGFP) (5-moUTP, #R1016), firefly luciferase (Fluc) mRNA (mFluc) (5-moUTP, #R1013), Cyanine5 labeled mFluc (Cy5-mFluc) (5-moUTP, #R1010), Cell Counting Kit-8 (CCK-8), and d-fluorescein (potassium salt) were obtained from APE×Bio Co., Ltd. (America). Carboxyfluorescein labeled small interfering RNA (FAM-siRNA) was purchased from OLIGOBIO Co., Ltd. (China). DNA was obtained from GENEWIZ (America). Trypsin-EDTA (0.25%), Penicillin-Streptomycin, Dulbecco's modified phosphate-buffered saline (PBS), MEM (Minimum Essential Medium) and DMEM (Dulbecco's Modified Eagle Medium) were purchased from Thermo Fisher Scientific. Ham's F-12K Medium (F12K) was obtained from Cellverse Co., Ltd. (Shanghai, China). Fetal bovine serum (FBS) was obtained from NEWZERUM Co. Ltd. All other chemicals were purchased from J&K SCIENTIFIC (Beijing, China) and used without further purification.

Chemical lipidation of KHn. The lipidation of KHn was performed based on ring-opening nucleophilic substitution reactions between 1,2-epoxides and the aliphatic amines (from the N-terminals and the lysine side chains) and the imidazolyl groups (from the histidine side chains) on KHn (**Fig. S1**), as we previously reported.[1] Briefly, the KHn (0.5 mmol, 1 equiv) and 1,2-epoxide (3N equiv, where N is the number of primary aliphatic amines on KHn) were added to a heavy-wall pressure vessel containing 3 mL methanol (MeOH). After sealed, the reaction was heated to 90 °C with stirring for 3 d. The crude products were dialyzed (MWCO 300 Da) and freeze-dried for further experiments. The obtained KHn-based lipopeptide were denoted as KHn-LP or Ex/Ax-KHn.

Preparation of KHn/lipid composite carriers by physical mixing. KHn/lipid composite carriers were prepared by physically pipette mixing KHn aqueous solution (enzyme-free) with cationic lipid DOTAP ethanol solution at a molar ratio of KHn to DOTAP of 4:1, 3:2, 1:1, 2:3, and 1:4 respectively, and the composite carriers were denoted as KHn/DOTAP.

Preparation of the carrier@nucleic acid complexes. First, prepare the carrier stock solution, including KHn aqueous solution, DOTAP ethanol solution, KHn/DOTAP solution, and KHn-LP ethanol solution (enzyme-free). Also, prepare a 10 mM citrate buffer diluted nucleic acid stock solution (enzyme-free) at pH 3. Mix the carrier stock solution and the nucleic acid stock solution at a volume ratio of 1:3 using a

pipette, and then incubated at room temperature for 30 minutes. For KHn@nucleic acid complexes, the KHn-to-nucleic acid mass ratio is 30; for KHn/DOTAP@nucleic acid complexes, DOTAP@nucleic acid complexes and KHn-LP@nucleic acid complexes, the carrier-to-nucleic acid mass ratio is 10:1; for KHn-LP@nucleic acid complexes, the carrier-to-nucleic acid mass ratio is 10:1. For *in vivo* experiments, KHn/DOTAP@nucleic acid complexes, DOTAP@nucleic acid complexes and KHn-LP@nucleic acid complexes were further dialyzed against 1×PBS buffer in Pur-A-Lyzer chambers (Sigma-Aldrich, MWCO 3500 Da) for 1.5 h and were stored at 4 °C before injection. The Lipo 2000@nucleic acid complexes were prepared according to the manufacturer's instructions.

Gel electrophoretic mobility shift assay. A gel electrophoretic mobility shift assay was carried out to examine the nucleic acid encapsulation capacity of carriers. Add 6 μL of 6×DNA loading buffer (TransGen Biotech, China, #GH101-01) to the prepared carrier@DNA complexes, and then the complexes were loaded onto 2 % (w/v) agarose gel. The gel electrophoresis experiments were carried out at a voltage of 125 V, and the running time was 25 min. The gels were visualized under UV illumination.

Encapsulation efficiency (ee) tests. The mRNA ee of carriers used in this study was determined using RNA Quant Kit (Vazyme Biotech, China, #DD3511) according to the manufacturer's instructions. Specifically, the fluorescence emission intensity (excitation wavelength of 480 nm and emission wavelength of 520 nm) of total mRNA samples as well as prepared carrier@mRNA complexes, was measured using a multilabel reader (PerkinElmer, EnSpire), and the mRNA concentration of each sample was obtained against a standard curve. The ee was calculated using the following formula: ee % = (total mRNA - free mRNA) / (total mRNA) × 100%.

Dynamic light scattering (DLS) tests. The hydrodynamic size, polydispersity index (PDI), and Zeta potential of the prepared carrier@mRNA complexes (diluted tenfold with pH 7.4 1×PBS buffer) were measured three times at 25 °C using a Zetasizer Nano ZS90 set-up (Malvern Panalytical Instruments).

Transmission electron microscope (TEM). 6 μL of the prepared carrier@mRNA complexes (diluted twentyfold with pH 7.4 1×PBS buffer) was directly dripped onto the surface of the copper grid and left at room temperature overnight without stained. The JEM-1400Flash transmission electron microscope or JEM-2100F field emission transmission electron microscope (JEOL Ltd., Japan) was used to image the samples.

Cell culture and animal studies. Hela (human cervical cancer cells), A549 (human lung cancer cells), CHO (Chinese hamster ovary cells), DC 2.4 (mouse bone marrow-derived dendritic cells), PC 12 (rat

adrenal gland pheochromocytoma cells), Vero (African Green monkey renal cells) were obtained from Pricella Biotechnology Co., Ltd. (China) and were cultured in complete DMEM, F12K, or MEM (with 10% FBS and 0.5% penicillin/streptomycin) according to manufacturer's instructions. The cells were cultured at 37 °C in an incubator with 5 % CO_2, and routinely tested for mycoplasma contamination.
C57BL/6 female mice (6-8 weeks, 18-20 g) were purchased from SPF Biotechnology Co. Ltd. (Beijing, China). Mice were maintained in a barrier facility with a 12 h light/12 h dark cycle, at ≈ 20 °C and 40% humidity.

CCK-8 cytotoxicity assay. The cytotoxicity of the carriers was evaluated using the CCK-8. Cells were seeded at a density of 5.0×10^3 cells per well in a 96-well plate and incubated at 37 °C for 24 h, and then treated with carriers at a certain concentration in complete medium. Next, the cells were further incubated at 37 °C for an additional 48 h. Subsequently, 10 μL of CCK-8 solution was added to each well, and after a 2 h incubation, the absorbance at 450 nm was measured at 25 °C using an EnSpire microplate reader. Three replicate experiments were conducted for each sample.

Cellular uptake experiments. Cells were seeded at a density of 5.0×10^4 cells per well in a 24-well plate. 24 h later, the prepared carrier@FAM-siRNA complexes were diluted to 500 μL with MEM and used to treat the cells (1 μg FAM-siRNA per well). After 4 h, the carrier@FAM-siRNA complexes were removed. Then, the level of FAM-siRNA uptake by cells was observed by inverted fluorescence microscopy (Olympus IX73) and measured by flow cytometry (BD Biosciences, America).

Confocal laser scanning microscopy (CLSM). A549 cells were seeded in the 2 cm diameter Thermo Scientific Nunc petri dish with a glass bottom at a density of 2.0×10^5 cells per dish. 24 h later, the prepared carrier@FAM-siRNA complexes were diluted to 2 mL with MEM and used to treat the A549 (3 μg FAM-siRNA per dish). After 3 h, the carrier@FAM-siRNA complexes were removed. Cells were washed 3 times with 1× PBS and treated with complete medium containing Lyso-Tracker Red for 1 h and fixed with 4% paraformaldehyde for 10 min. Then, cells were washed 3 times with 1×PBS and nucleus were stained with 4',6-diamidino-2'-phenylindole (DAPI) for 3 min. After washing the cells three times with 1×PBS, cover them with complete medium. Finally, the cells were observed on Super-resolution confocal microscopy (Leica SP8) with a 63 × oil lens.

***In vitro* mEGFP delivery.** Cells were seeded at a density of 5.0×10^4 cells per well in a 24-well plate. 24 h later, the prepared carrier@mEGFP complexes were diluted to 500 μL with MEM and used to treat the cells (1 μg mEGFP per well). After 4 h, the carrier@mEGFP complexes were removed and replaced with a fresh complete medium, and the cells continued to incubate for 48 h. Then, the EGFP expression was

observed using an inverted fluorescence microscope, and the positive rate of cells expressing EGFP was measured and analyzed by flow cytometry and FlowJo software.

***In vitro* mFluc delivery.** Cells were seeded at a density of 1.0×10^4 cells per well in a black 96-well plate with a transparent bottom. 24 h later, the prepared carrier@mFluc complexes were diluted to 100 μL with MEM and used to treat the cells (50 ng mFluc per well). After 4 h, the carrier@mFluc complexes were removed and replaced with a fresh complete medium, and the cells continued to incubate for 48h. Then, the Fluc expression was evaluated by a Fluc assay kit according to the manufacturer's instructions (GenScript, America, #L00877C).

***In vivo* biodistribution.** The prepared carrier@Cy5-mFluc complexes were intravenously (*i.v.*) injected into C57BL/6 mice (the dose was 0.75 mg kg^{-1}). 2 h later, fluorescence imaging of the isolated organs (heart, liver, spleen, lung, and kidney) was performed on an IVIS imaging system (Perkin Elmer). 1×PBS was set as the negative control.

***In vivo* organ-targeted mFLuc delivery.** The prepared carrier@mFluc complexes were *i.v.* injected into C57BL/6 mice (the dose was 0.75 mg kg^{-1}). After 6 h, mice were intraperitoneally injected with 200 μL d-luciferin (potassium salt) (20 mg mL^{-1} in 1×PBS). 15 min later, bioluminescence imaging of the live mice and their isolated organs (heart, liver, spleen, lung, and kidney) was performed on an IVIS imaging system. 1×PBS was set as the negative control.

Supplementary Figures

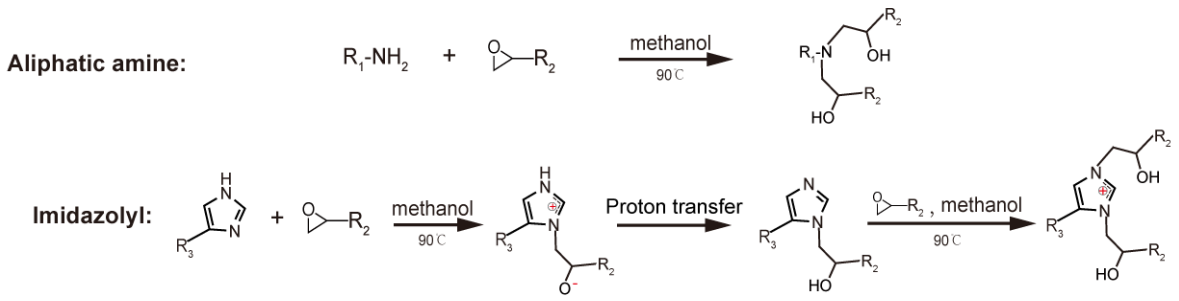

Fig. S1 Ring-opening reaction processes of 1, 2-epoxides with aliphatic amines and imidazolyl groups on KHn in this work.[2, 3] The more basic the groups are, the easier they are to perform ring-opening substitution reactions with 1, 2-epoxides. Since the basicity of aliphatic amines is stronger than that of imidazolyl groups, aliphatic amines preferentially react with 1, 2-epoxides, followed by imidazolyl groups.[4-6]

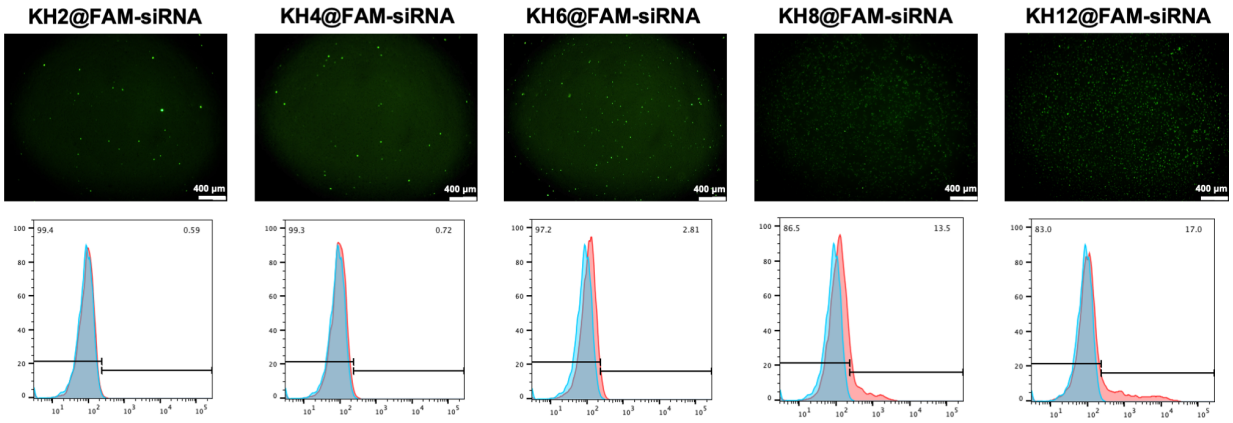

Fig. S2 The inverted fluorescence microscope images (top) and corresponding flow cytometry characterization results (bottom) of Hela treated with KHn@FAM-siRNA complexes for 4 h.

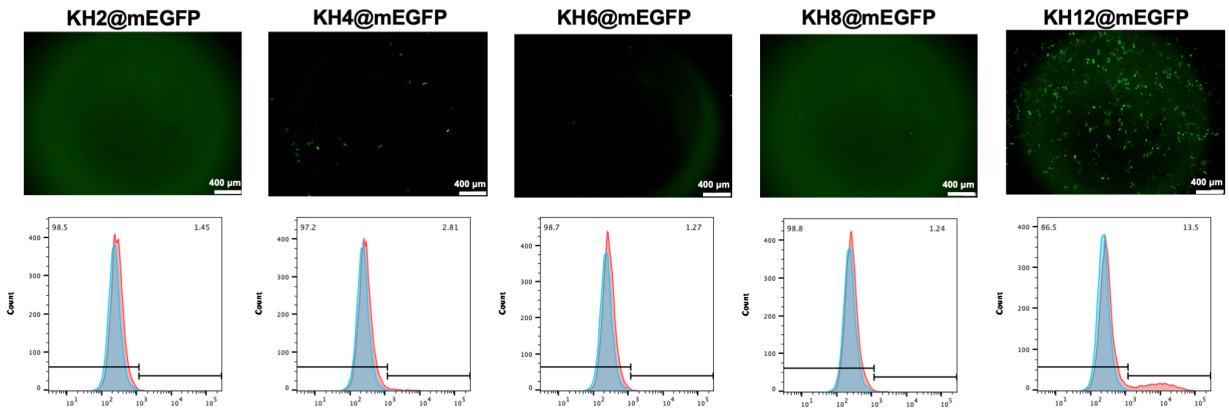

Fig. S3 The inverted fluorescence microscope images (top) and corresponding flow cytometry characterization results (bottom) of Hela treated with KHn@mEGFP complexes after 48 h.

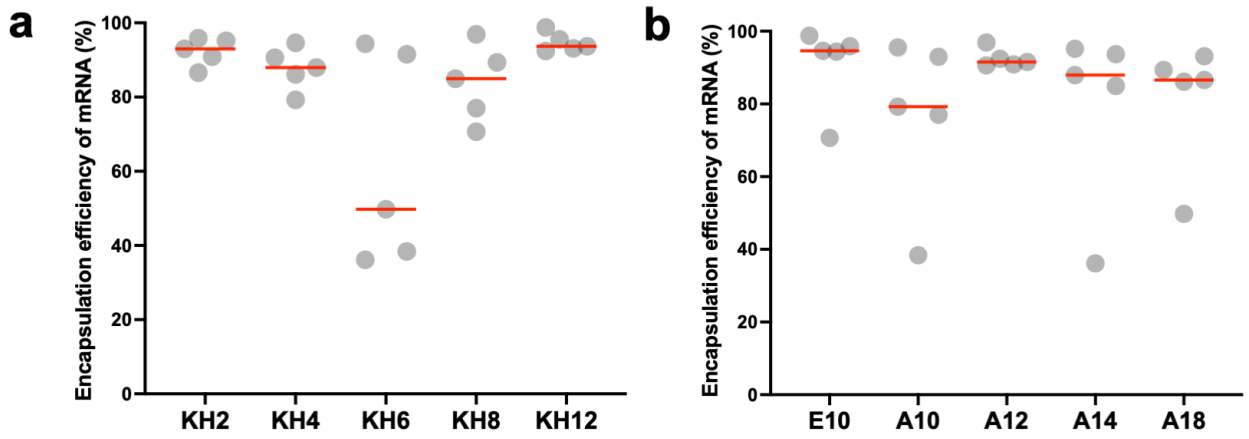

Fig. S4 (a-b) The mRNA encapsulation efficiency of KHn-LP was re-summarized based on KHn-LP headgroups (KH2, KH4, KH6, KH8, and KH12) (a) and tails (E10, A10, A12, A14, and A18) (b), respectively (n =3).

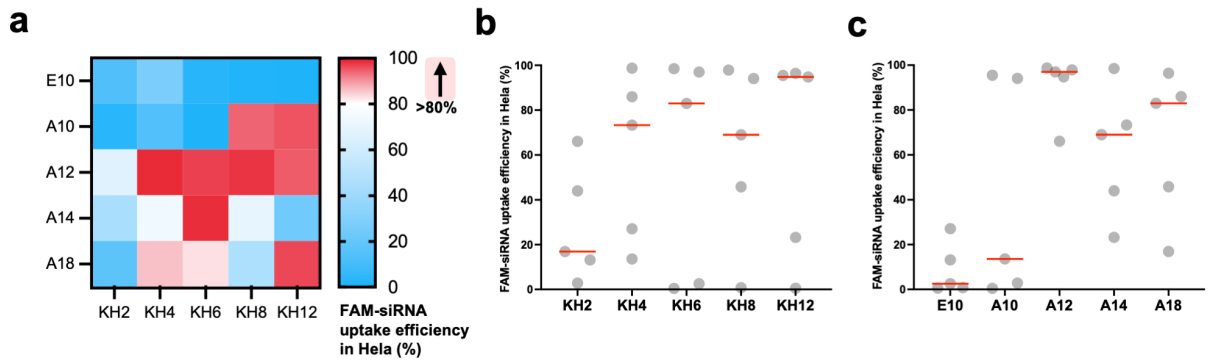

Fig. S5 (a) A heatmap of the uptake efficiency of KHn-LP@FAM-siRNA complexes in Hela treated for 4 h (n=2). (b-c) The Hela uptake efficiency of KHn-LP@FAM-siRNA complexes was re-summarized based on KHn-LP headgroups (KH2, KH4, KH6, KH8, and KH12) (a) and tails (E10, A10, A12, A14, and A18) (b), respectively (n =2).

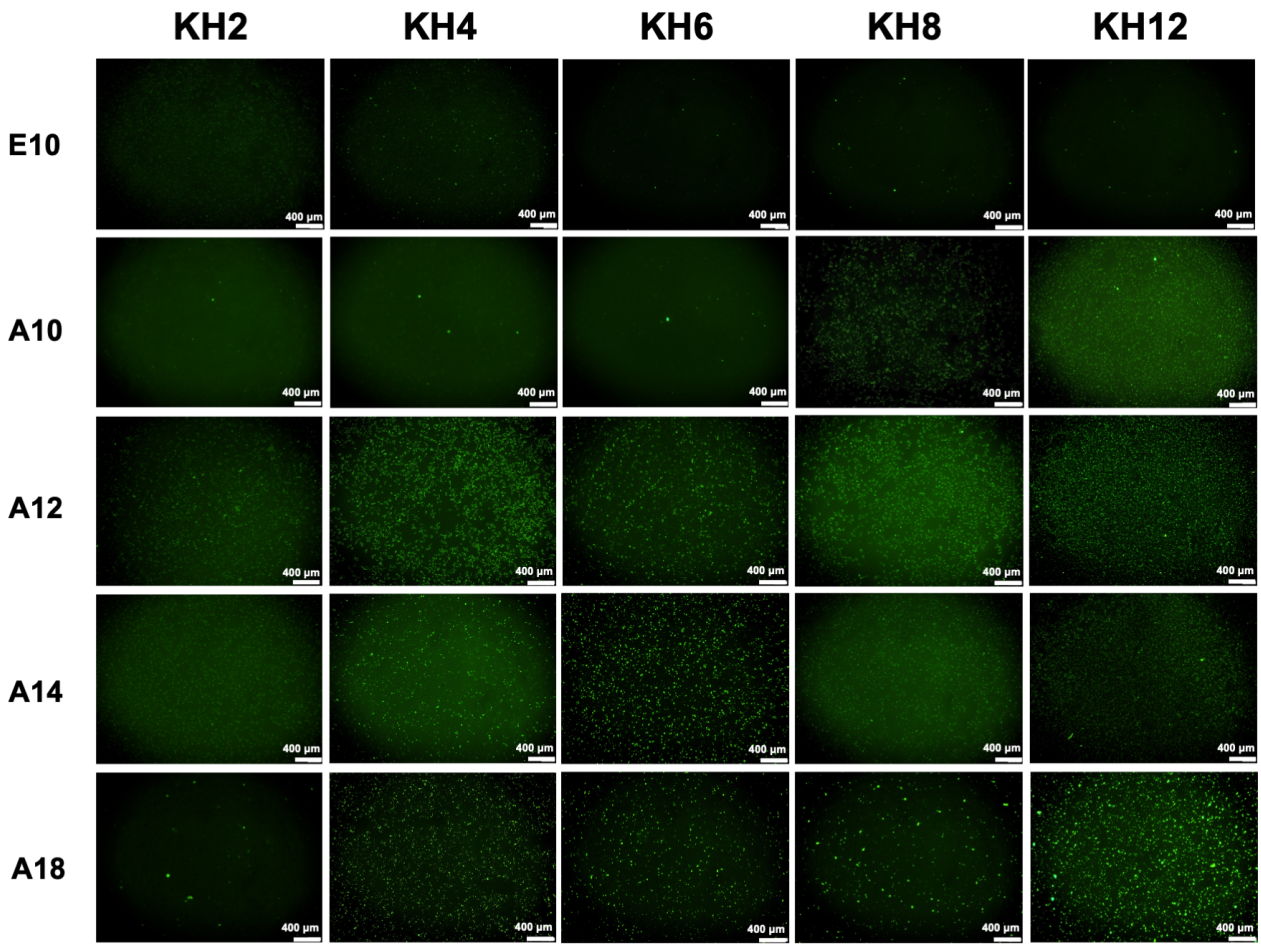

Fig. S6 The inverted fluorescence microscope images of Hela treated with KHn-LP@FAM-siRNA complexes after 4 h.

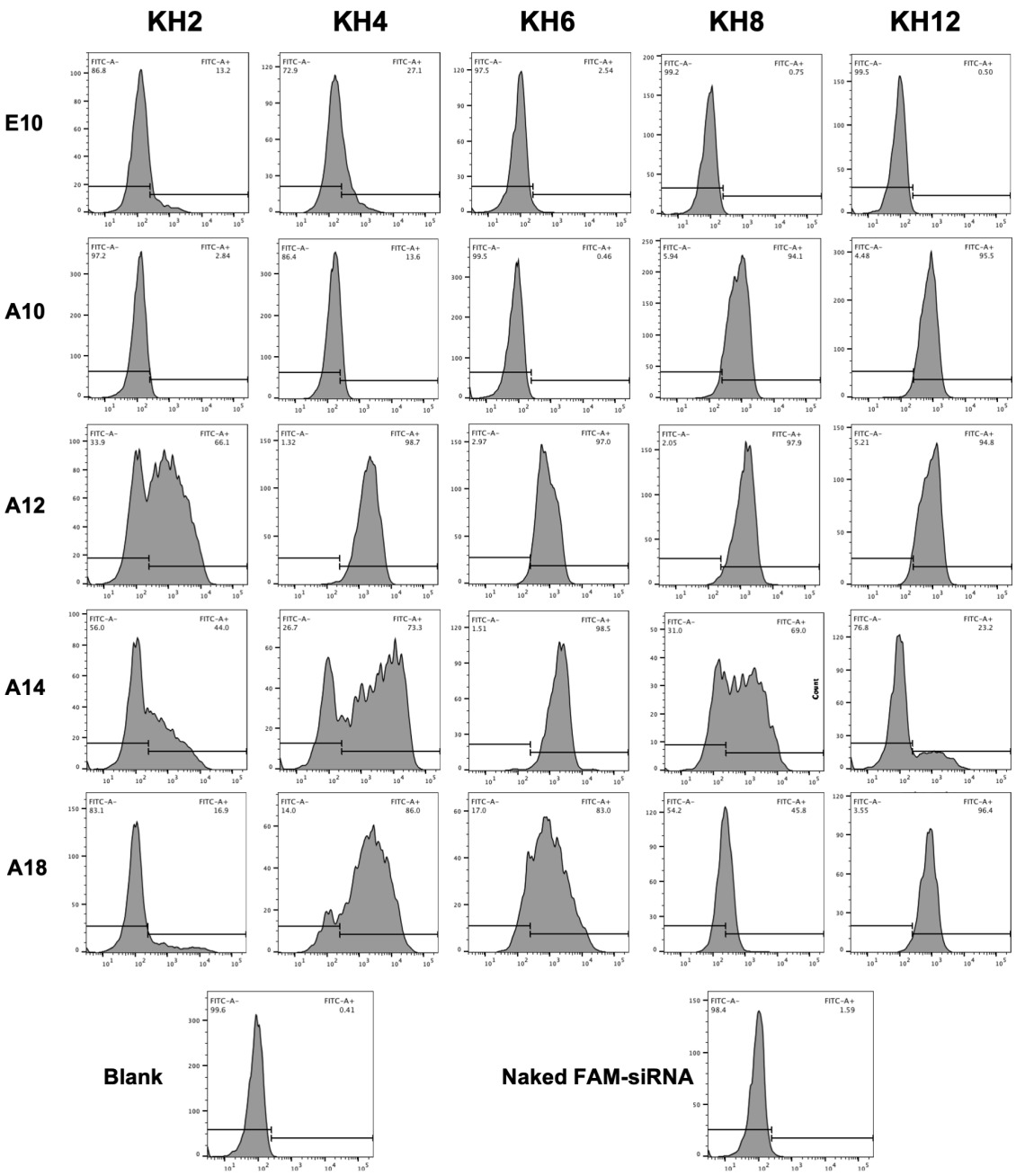

Fig. S7 The flow cytometry characterization results of Hela treated with KHn-LP@FAM-siRNA complexes after 4 h.

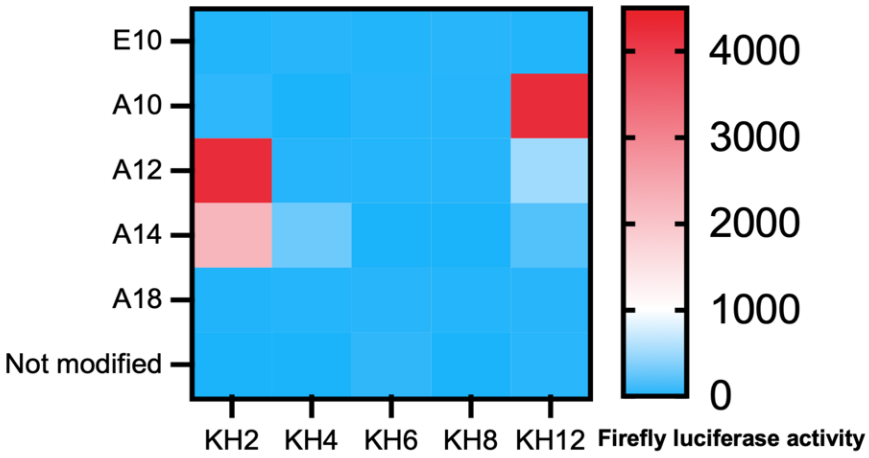

Fig. S8 A heatmap of the firefly luciferase activity of A549 treated with KHn-LP@mFluc and KHn@mFluc complexes after 48 h (n=2).

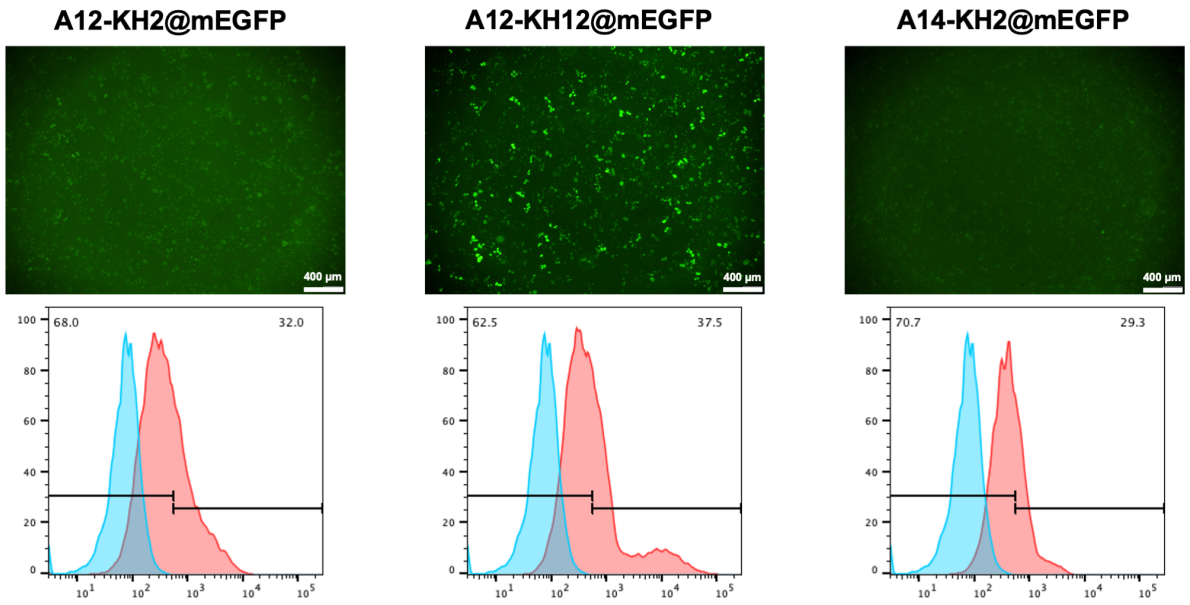

Fig. S9 The inverted fluorescence microscope images (top) and corresponding flow cytometry characterization results (bottom) of Hela treated with A12-KH2@mEGFP, A12-KH12@mEGFP, and A14-KH2@mEGFP complexes (from left to right) after 48 h.

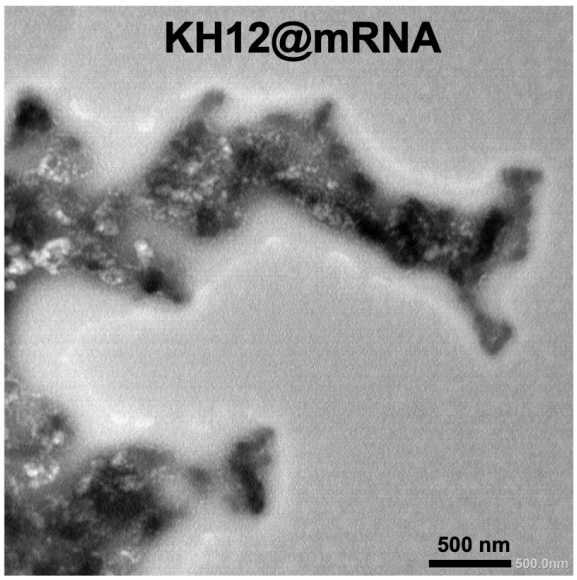

Fig. S10 The TEM image of KH12@mRNA complexes at neutral pH.

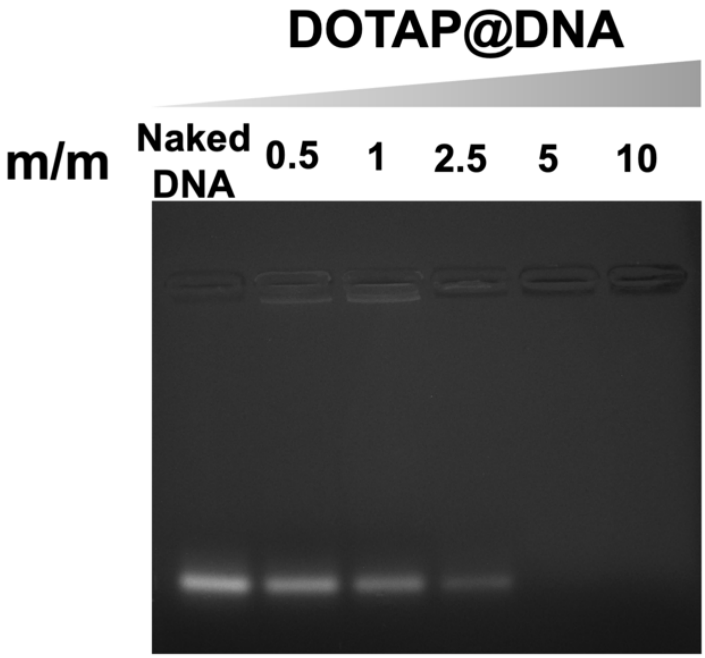

Fig. S11 Gel electrophoresis effects of DOTAP@DNA complexes at different DOTAP-to-DNA mass ratios (0.5, 1, 2.5, 5, and 10).

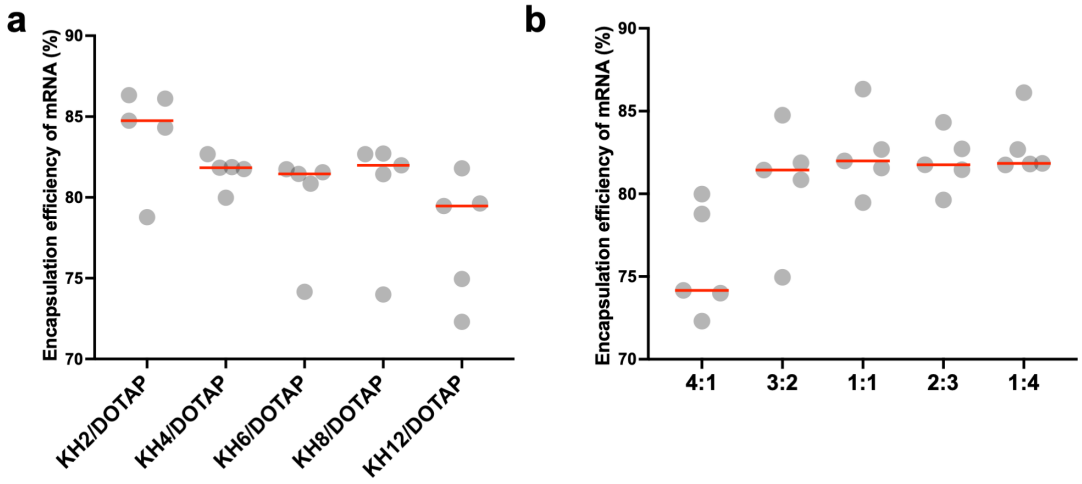

Fig. S12 (a-b) The mRNA encapsulation efficiency of KHn/DOTAP was re-summarized based on different KHn/DOTAP systems (KH2/DOTAP, KH4/DOTAP, KH6/DOTAP, KH8/DOTAP, and KH12/DOTAP) (a) and KHn-to-DOTAP molar ratios (1:0, 4:1, 3:2, 1:1, 2:3, and 1:4) (b), respectively (n =3).

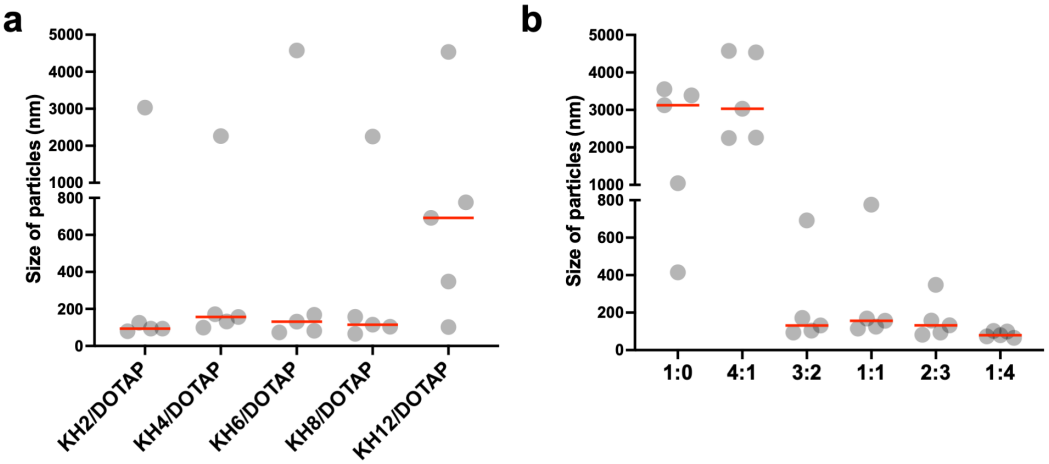

Fig. S13 (a-b) The particle size of KHn/DOTAP@mRNA complexes was re-summarized based on different KHn/DOTAP systems (KH2/DOTAP, KH4/DOTAP, KH6/DOTAP, KH8/DOTAP, and KH12/DOTAP) (a) and KHn-to-DOTAP molar ratios (1:0, 4:1, 3:2, 1:1, 2:3, and 1:4) (b), respectively (n =3).

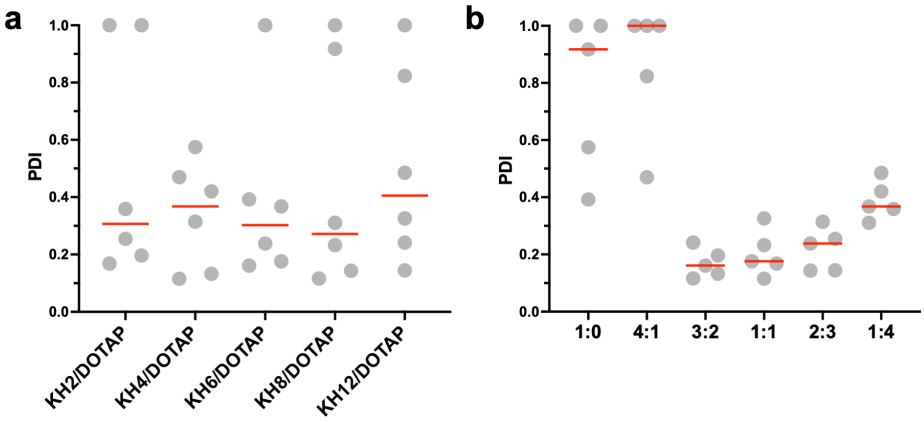

Fig. S14 (a-b) The PDI of KHn/DOTAP@mRNA complexes was re-summarized based on different KHn/DOTAP systems (KH2/DOTAP, KH4/DOTAP, KH6/DOTAP, KH8/DOTAP, and KH12/DOTAP) (a) and KHn-to-DOTAP molar ratios (1:0, 4:1, 3:2, 1:1, 2:3, and 1:4) (b), respectively (n =3).

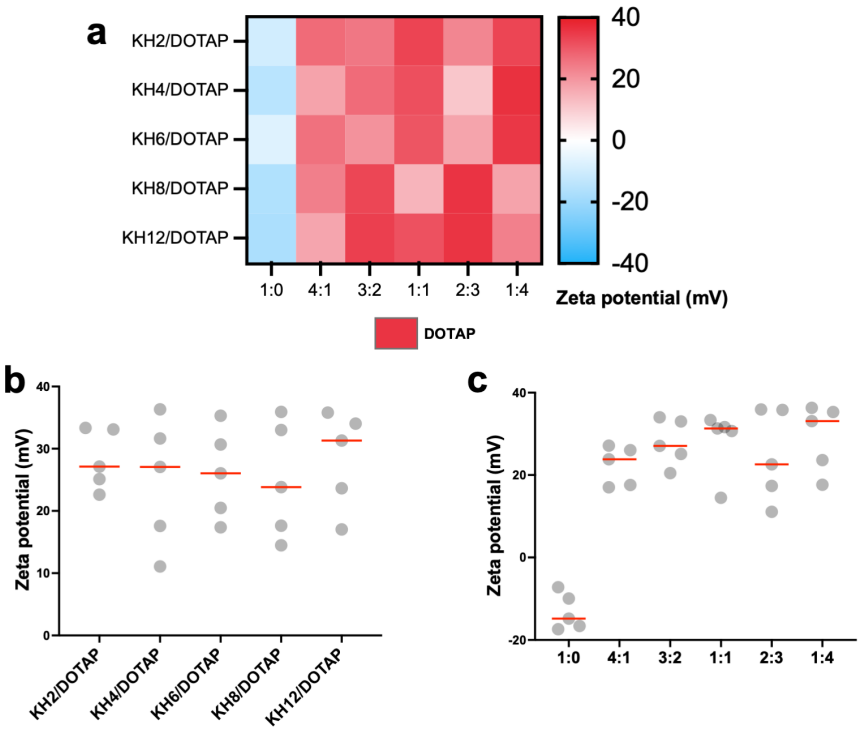

Fig. S15 (a) A heatmap of the zeta potential of the KHn/DOTAP@mRNA complexes with different KHn-to-DOTAP molar ratios (1:0, 4:1, 3:2, 1:1, 2:3, and 1:4) (n=3). DOTAP@mEGFP complexes were used as a control. (b-c) The zeta potential of KHn/DOTAP@mRNA complexes was re-summarized based on different KHn/DOTAP systems (KH2/DOTAP, KH4/DOTAP, KH6/DOTAP, KH8/DOTAP, and KH12/DOTAP) (b) and KHn-to-DOTAP molar ratios (1:0, 4:1, 3:2, 1:1, 2:3, and 1:4) (c), respectively (n =3).

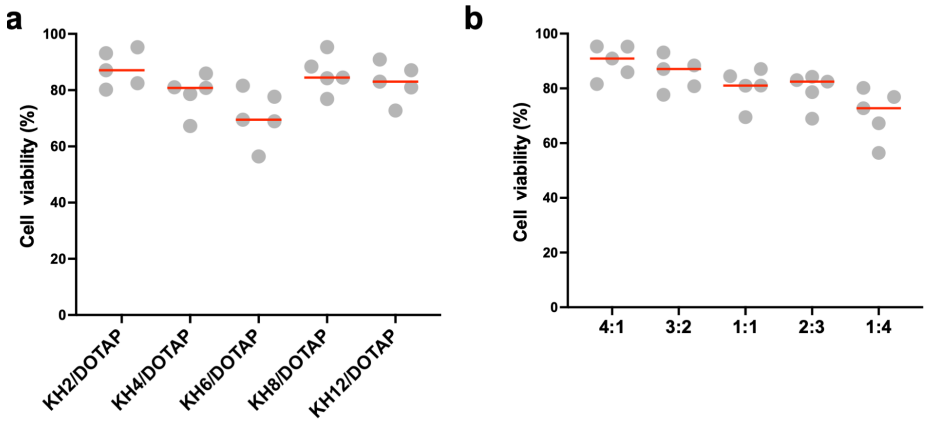

Fig. S16 (a-b) The cell viability of Hela treated with the KHn/DOTAP@mRNA complexes (concentration of 20 μg/mL, 48 h) was re-summarized based on different KHn/DOTAP systems (KH2/DOTAP, KH4/DOTAP, KH6/DOTAP, KH8/DOTAP, and KH12/DOTAP) (a) and KHn-to-DOTAP molar ratios (1:0, 4:1, 3:2, 1:1, 2:3, and 1:4) (b), respectively (n =3).

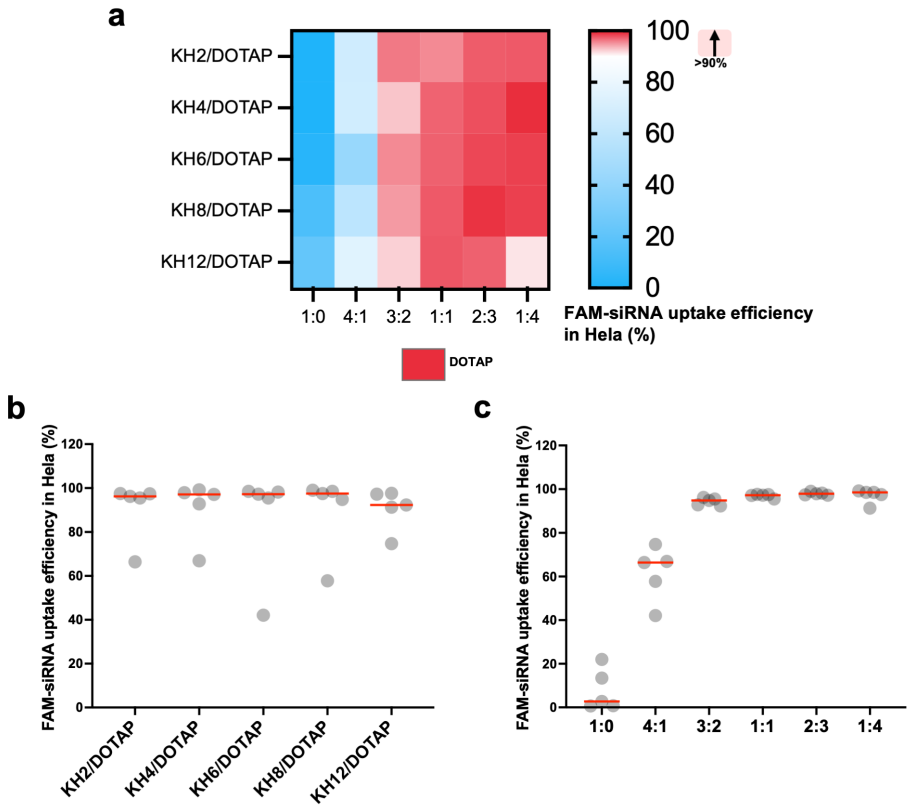

Fig. S17 (a) A heatmap of the uptake efficiency of KHn/DOTAP@FAM-siRNA complexes in Hela treated for 4 h (n=2). DOTAP@ FAM-siRNA complexes were used as a control. (b-c) The uptake efficiency of KHn/DOTAP@mRNA complexes was re-summarized based on different KHn/DOTAP systems (KH2/DOTAP, KH4/DOTAP, KH6/DOTAP, KH8/DOTAP, and KH12/DOTAP) (b) and KHn-to-DOTAP molar ratios (1:0, 4:1, 3:2, 1:1, 2:3, and 1:4) (c), respectively (n =2).

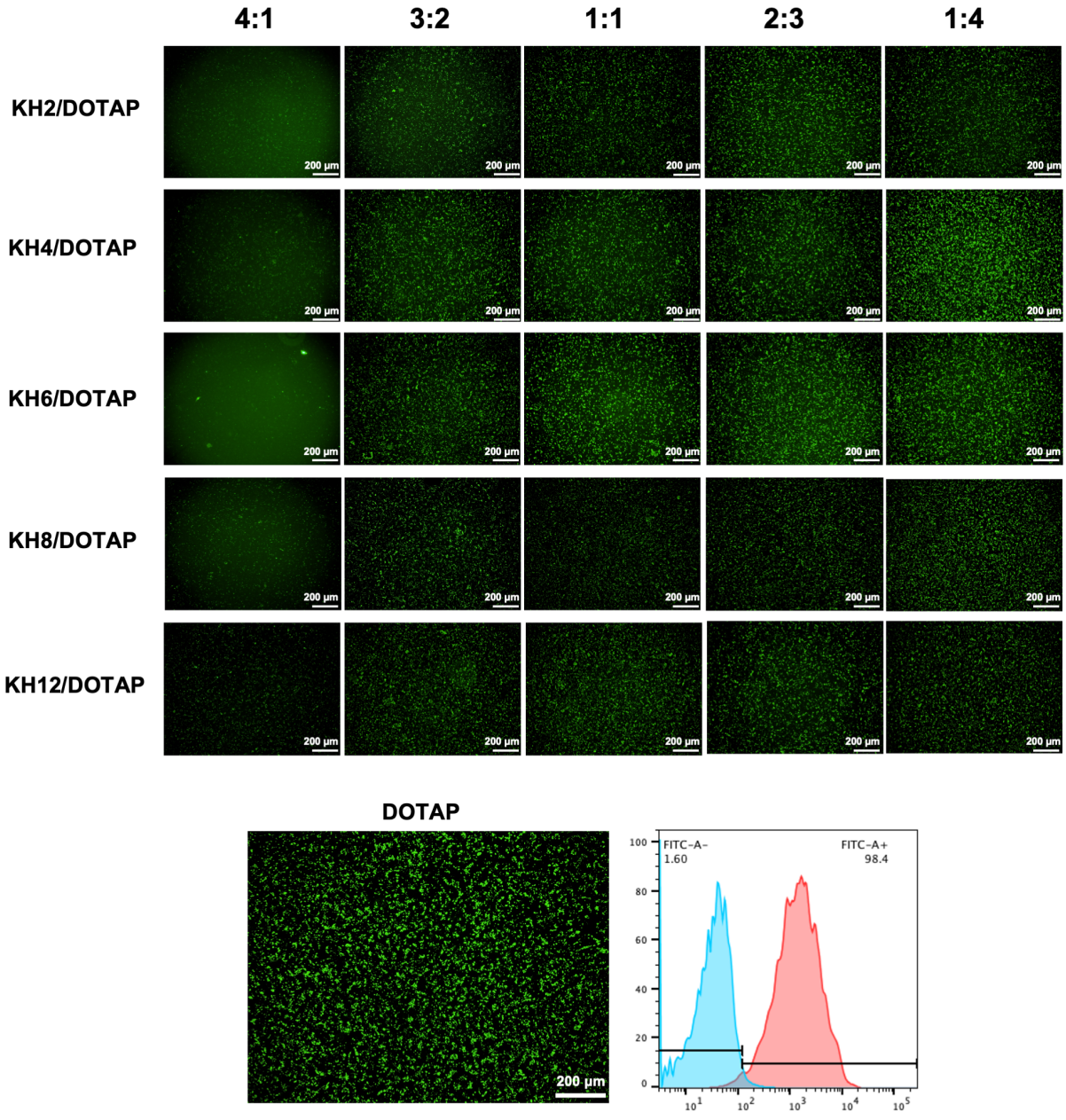

Fig. S18 The inverted fluorescence microscope images of Hela treated with KHn/DOTAP@FAM-siRNA complexes after 4 h. DOTAP@ FAM-siRNA complexes were used as a control.

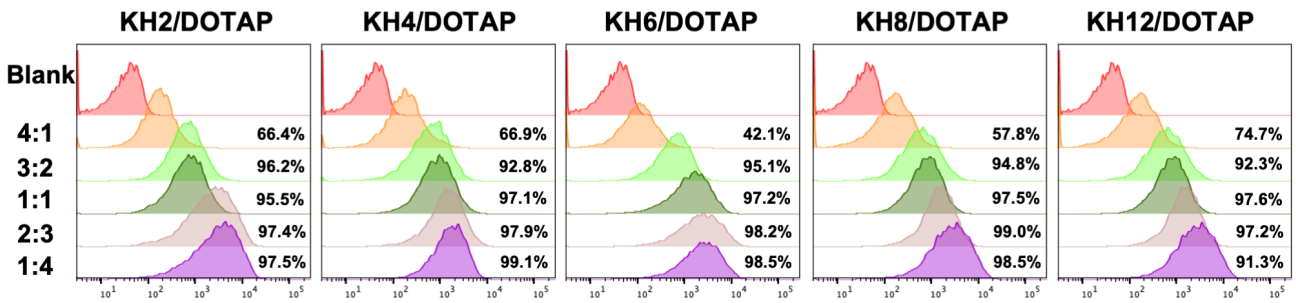

Fig. S19 The flow cytometry characterization results of Hela treated with KHn/DOTAP@FAM-siRNA complexes after 4 h. DOTAP@ FAM-siRNA complexes were used as a control.

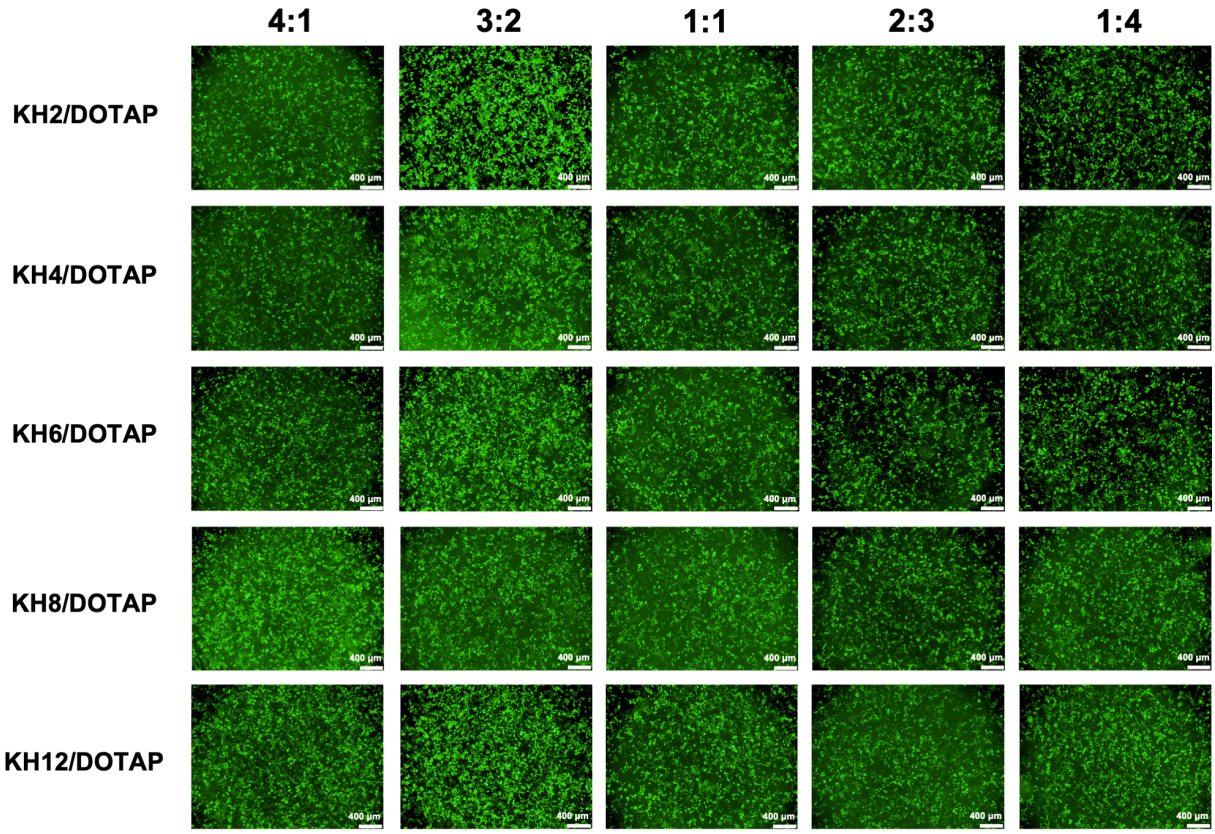

Fig. S20 The inverted fluorescence microscope images of Hela treated with KHn/DOTAP@mEGFP complexes with different KHn-to-DOTAP molar ratios (1:4, 2:3, 1:1, 3:2, and 4:1) after 48 h.

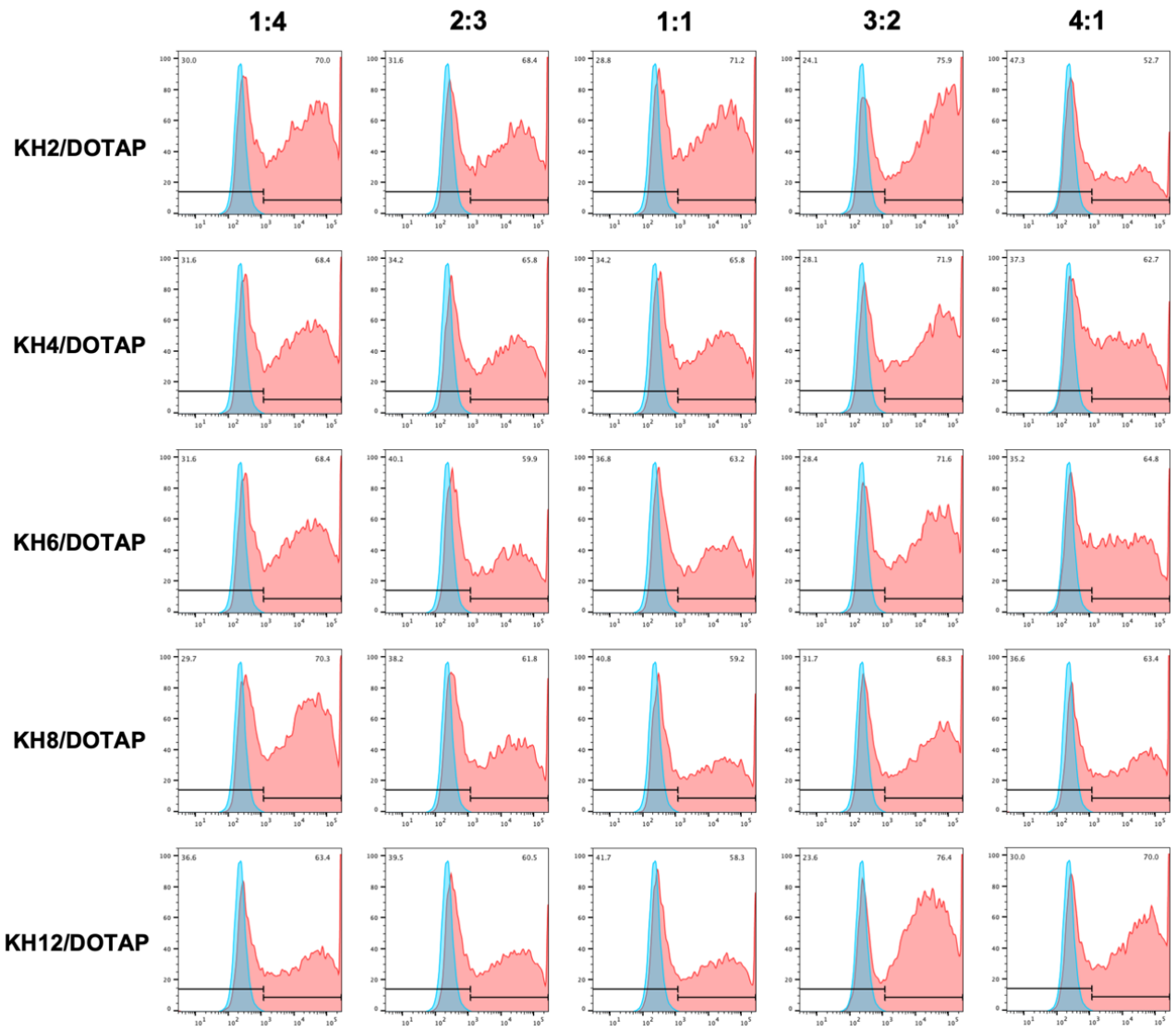

Fig. S21 The flow cytometry characterization results of Hela treated with KHn/DOTAP@mEGFP complexes with different KHn-to-DOTAP molar ratios (1:4, 2:3, 1:1, 3:2, and 4:1) after 48 h.

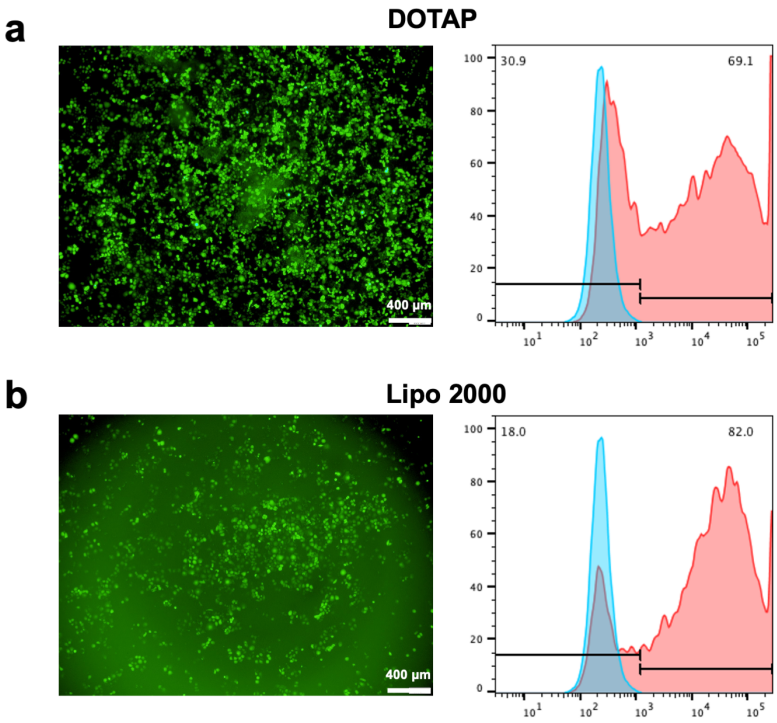

Fig. S22 The inverted fluorescence microscope images (left) and corresponding flow cytometry characterization results (right) of Hela treated with (a) DOTAP@EGFP and (b) Lipo 2000@mEGFP complexes after 48h.

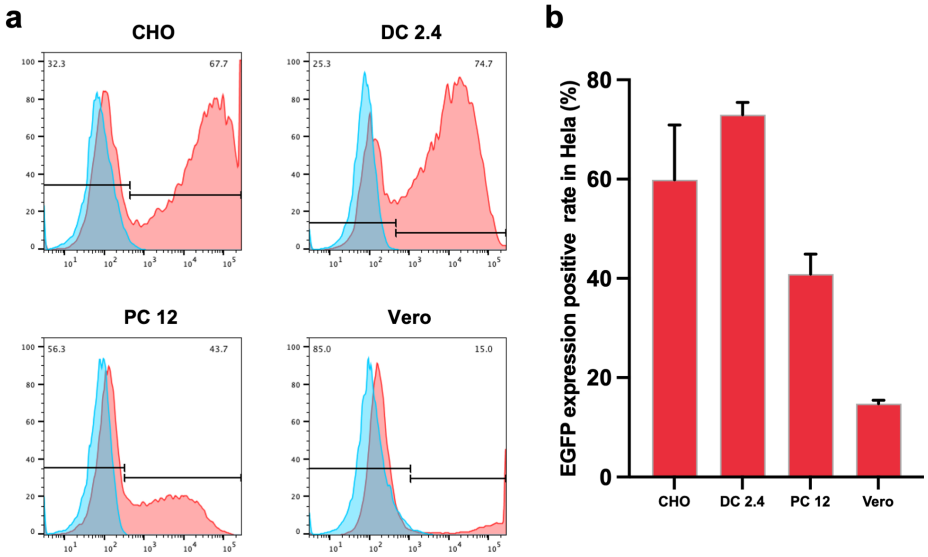

Fig. S23 (a) The flow cytometry characterization results of CHO, DC 2.4, PC 12, and Vero treated with KH2/DOTAP$_{3:2}$@mEGFP complexes after 48 h. (b) The statistical EGFP expression positive rate of CHO, DC 2.4, PC 12, and Vero treated with KH2/DOTAP$_{3:2}$@mEGFP complexes after 48 h (n=2 or 3).

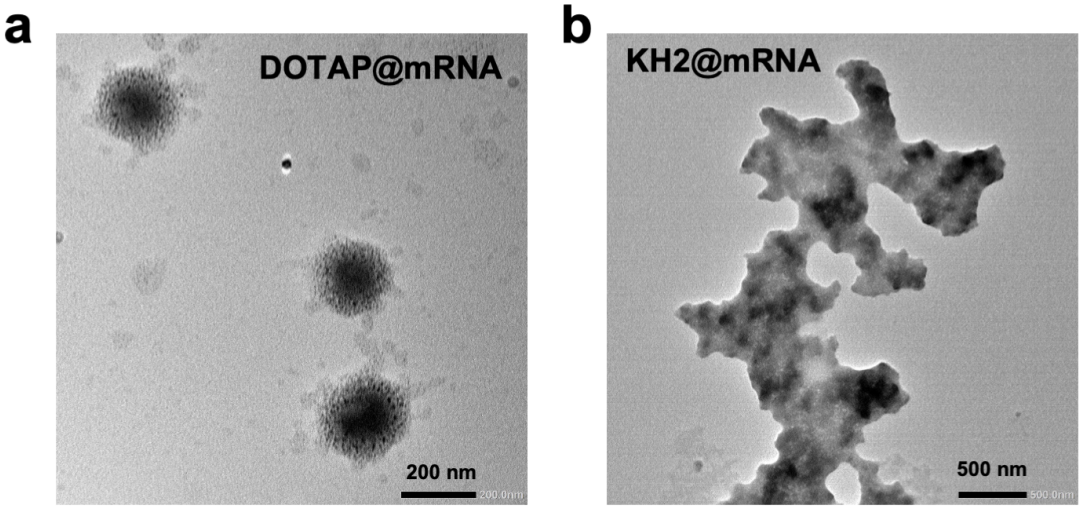

Fig. S24 The TEM images of (a) DOTAP@mRNA and (b) KH2@mRNA complexes at neutral pH.

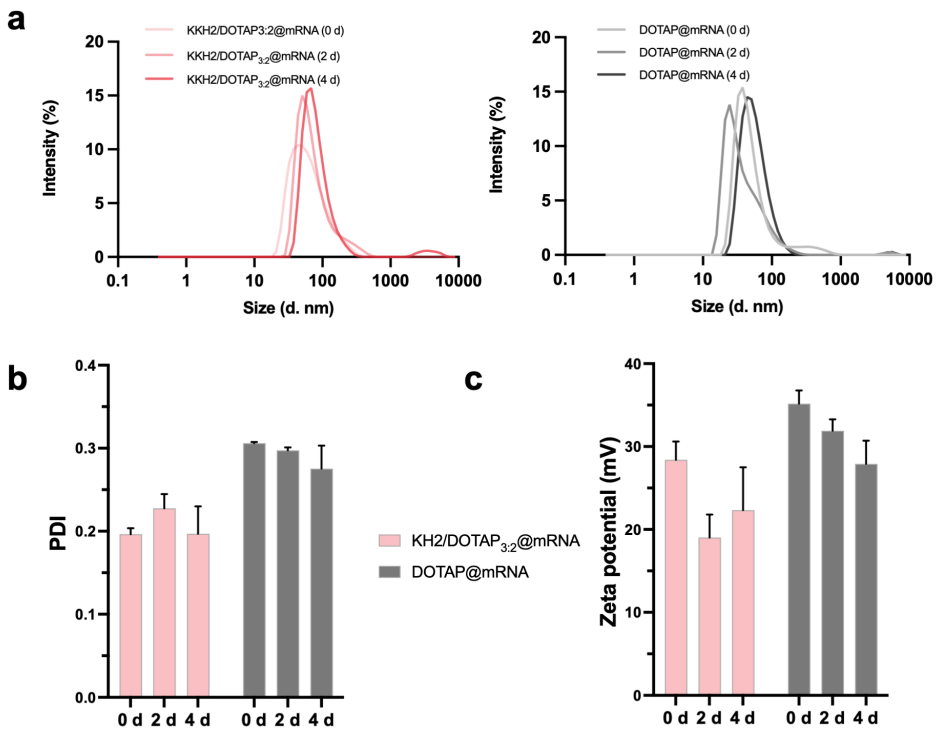

Fig. S25 (a-c) Hydrodynamic diameter (a), PDI (b), and zeta potential (c) of the KH2/DOTAP$_{3:2}$@mRNA complexes and DOTAP@mRNA complexes stored at 4°C, pH 7, for 0d, 2d, and 4d, respectively (n=3).

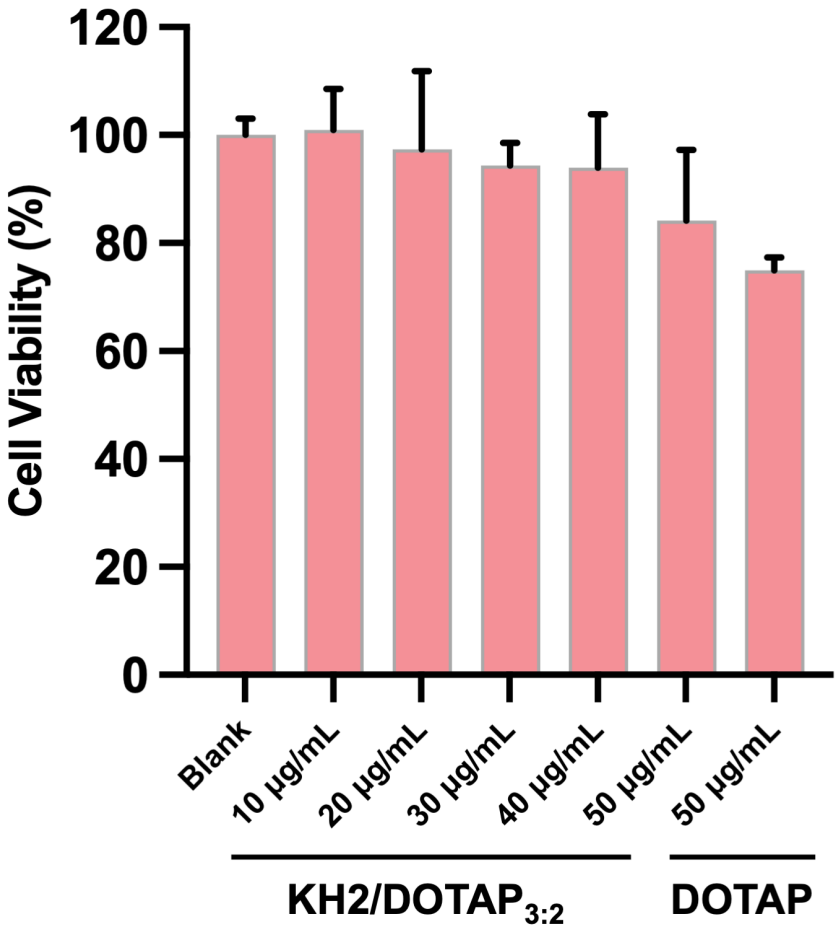

Fig. S26 Cell viability of Hela treated with different KH2/DOTAP$_{3:2}$ complexes concentrations of 10, 20, 30, 40, and 50 μg/mL and with a DOTAP concentration of 50 μg/mL for 48 h (n=3).

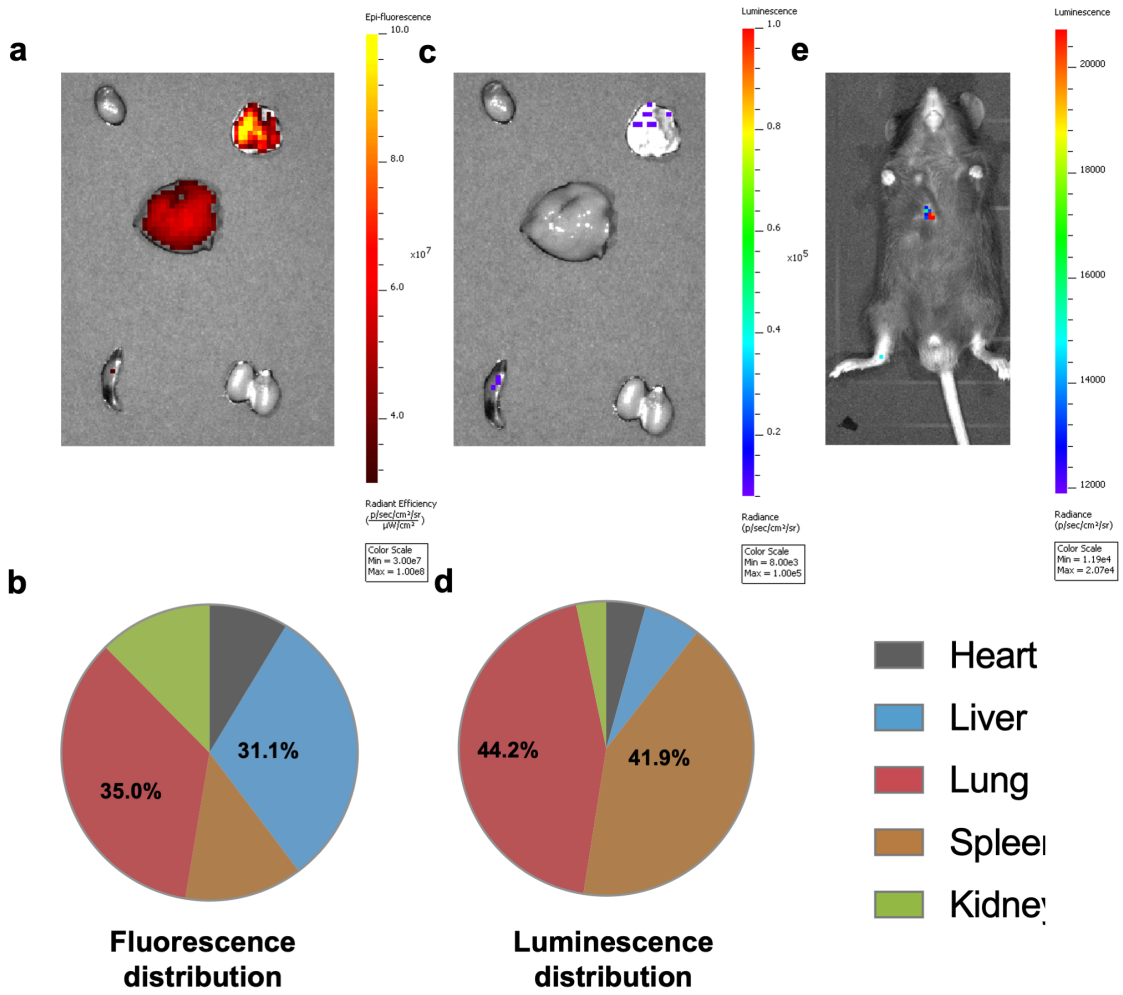

Fig. S27 (a) Fluorescenceimaging of major organs after DOTAP-mediated delivery of Cy5-mFluc (*i.v.*, 0.75 mg kg^{-1}, 2h, n = 3 biologically independent animals). (b) Pie chart based on the average radiance statistics showing the proportional fluorescence distribution across major organs after DOTAP-mediated systemic Cy5-mFluc delivery (*i.v*, 0.75 mg kg^{-1}, 2 h, n = 3 biologically independent animals). (c) Bioluminescence imaging of major organs after DOTAP-mediated delivery of mFluc (*i.v.*, 0.75 mg kg^{-1}, 6 h, n = 3 biologically independent animals). (d) Pie chart based on the average radiance statistics showing the bioluminescence distribution across major organs after DOTAP-mediated systemic mFluc delivery (*i.v*, 0.75 mg kg^{-1}, 6 h, n = 3 biologically independent animals). (e) Bioluminescence imaging of live mice after KH2/DOTAP-mediated systemic delivery of mFluc (*i.v.*, 0.75 mg kg^{-1}, 6 h, n = 3 biologically independent animals).

Supplementary Tables

Table S1. The information of designed KHn.

Sequences	Abbreviations	Molecular weight (g/mol)	Net charge (pH=7.0)
KH-NH_2	KH2	282.18	2.21
KKHH-NH_2	KH4	547.33	3.25
KKKHHH-NH_2	KH6	812.49	4.68
KKKKHHHH-NH_2	KH8	1077.64	5.92
KHHKHHKHHKHH-NH_2	KH12	1625.88	6.86

Table S2. The comparison of in vitro mRNA transfection efficiency between the carriers used in this study and those reported in other studies.

Carrier system	Carrier name	Nucleic acid	Cell lines and transfection efficiency	Ref.
Lipopeptide	A10-KH12	EGFP mRNA	Hela: 71.2 %	This study
Peptide/lipid	KH2/DOTAP	EGFP mRNA	Hela: 75.9%	This study
Peptide/lipid	C14/DOPE+30% Chol-Pep 35	EGFP mRNA	B16-F10: ~25%	[7]
Peptide/Lipid	KKKKHHHHLLLLLLLL (KHL)/DOTAP	EGFP mRNA	HEK 293T: 80.1%	[8]
Lipopeptide/lipid	R5H5C-DOPE LNPs	EGFP mRNA	HepG2: 74.8%	[9]
PEGylated peptide	$PEG_{12}LA$	EGFP mRNA	HepG2: ~74.8%	[10]
LipoPepetide	DSPE-KK_2	siRNA	PC-3: ~70%	[11]
Peptide	BAP-V7	EGFP mRNA	Hela: ~27%	[12]
Peptide	LAH4-A1-Tyr2 (28 amino acids)	GFP mRNA	HEK293T: 71.4%	[13]

References

1. C. M. Tang, Y. X. Zhang, B. W. Li, X. W. Fan, Z. X. Wang, R. X. Su, W. Qi and Y. F. Wang, *Adv. Mater.*, 2025, **37**, 2415643.
2. F. L. Jin, X. Li and S. J. Park, *J. Ind. Eng. Chem.*, 2015, **29**, 1-11.
3. H. L. Gou, Y. Y. Zhao, Y. L. Zhou, W. Wei, X. M. Fei, X. J. Li and X. Y. Liu, *Polym. Adv. Technol.*, 2022, **33**, 610-626.
4. B. R. Moser, S. C. Cermak, K. M. Doll, J. A. Kenar and B. K. Sharma, *J. Am. Oil Chem. Soc.*, 2022, **99**, 801-842.
5. F. A. Saddique, A. F. Zahoor, S. Faiz, S. A. R. Naqvi, M. Usman and M. Ahmad, *Synth. Commun.*, 2016, **46**, 831-868.
6. R. Torregrosa, I. M. Pastor and M. Yus, *Tetrahedron*, 2007, **63**, 469-473.
7. D. Grant-Serroukh, M. R. Hunter, R. Maeshima, A. D. Tagalakis, A. M. Aldossary, N. Allahham, G. R. Williams, M. Edbrooke, A. Desai and S. L. Hart, *J. Control. Release*, 2022, **348**, 786-797.
8. J. J. Zhang, Z. X. Wang, J. W. Min, X. L. Zhang, R. X. Su, Y. F. Wang and W. Qi, *Langmuir*, 2023, **39**, 7484-7494.
9. H. Xiao, B. L. Feng, D. D. Gao, S. N. Shi, Y. Q. Yang, Y. W. Zhang, F. Y. Wang, Q. Yao, H. Q. Song, Y. Liu and G. Cheng, *Bioact. Mater.*, 2025, **54**, 829-849.
10. Y. Xu, Y. Zheng, X. Ding, C. Wang, B. Hua, S. Hong, X. Huang, J. Lin, P. Zhang and W. Chen, *Drug Deliv.*, 2023, **30**, 2219870.
11. Y. W. Dong, Y. Chen, D. D. Zhu, K. J. Shi, C. Ma, W. J. Zhang, P. Rocchi, L. Jiang and X. X. Liu, *J. Control. Release*, 2020, **322**, 416-425.
12. X. S. Yuan, S. Z. Luo and L. Chen, *Int. J. Pharm.*, 2022, **624**, 121983.
13. C. Dussouillez, M. Lointier, M. K. Sebane, S. Fournel, B. Bechinger and A. Kichler, *J. Pept. Sci.*, 2024, **30**, e3597.